Nanoporous Thin-film Waveguide Resonance Sensors with Wavelength Interrogation over a Broad Bandwidth

Z.-M. Qi*, Z. Zhang, Q. Liu and D.-F. Lu

State Key Laboratory of Transducer Technology, Institute of Electronics, Chinese Academy of Sciences, No. 19 Beisihuan West Road, Beijing 100190, China, zhimei-qi@mail.ie.ac.cn

ABSTRACT

A TiO_2 nanoporous thin film based leaky waveguide resonance sensor operating in the wavelength interrogation mode was characterized. The resonance wavelengths (λ_R) and the induced shifts in λ_R were determined directly from the reflected light intensity spectra measured at a given incident angle. A considerable broadening of the resonance band was observed with the sensor, mainly resulting from a large bulk scattering of the nanoporous TiO_2 film. The best fit to the experimental data with the Fresnel equations leads to a pore-volume fraction of 0.474 for the TiO_2 film. The sensor is responsive to adsorption of small molecules such as glutathione (GSH, MW = 307.3 Da). A change of the surrounding liquid from water to aqueous GSH solution (0.1 mM) results in a redshift of $\Delta\lambda_R \approx 3$ nm from λ_R = 593.6 nm, corresponding to a volume fraction of 0.05 for the GSH molecules adsorbed on the porous film based on simulations. According to the theoretical analyses, a small change in refractive index of the surrounding liquid can induce a large blueshift of λ_R under proper conditions.

Keywords: Nanoporous thin-film waveguides, resonance, wavelength interrogation, blue shift, high sensitivity

1 INTRODUCTION

Porous waveguide mode resonance (PWMR) sensors have recently attracted considerable attention because of their electromagnetic immunity, ultrahigh sensitivity, size dependent selectivity, real-time and label-free detection ability, and good compatibility with the electrochemical technique [1-5]. PWMR sensors usually have a similar geometry to a conventional surface plasmon resonance (SPR) sensor but are much more sensitive than the latter. The high sensitivity of PWMR sensors results from the strong interaction between the guided mode and the analyte molecules adsorbed inside the nanoporous waveguide. For SPR sensors with a naked gold film, the interaction of the evanescent wave with adsorbed target molecules occurs at the gold-layer/solution-sample interface, with an interaction depth as small as the molecular size, which leads to a limited sensitivity and consequently makes SPR sensors unable to directly detect small-molecule substances with molecular weight below 200 Da especially in the case of a low concentration [6]. In practice, a large variety of toxic, harmful and hazardous substances such as pesticides, cyanide, drugs, TNT, heavy metal ions, and volatile organic compounds are small molecules. They cannot be easily detected with SPR sensors. From the point of view of the trace detection of small molecules, PWMR sensors have the great advantage over SPR sensors, showing bright prospect as an alternative to SPR sensors. So far, PWMR sensors have been studied almost exclusively in the angular interrogation mode [1-4]. Our previous work shows the first example of a wavelength-interrogated PWMR sensor [5]. The PWMR sensor with wavelength interrogation allows for flexible adjustment of sensitivity and thus has a broad measurement range for the analyte concentrations. With a time-resolved CCD spectrometer the PWMR sensor can be used for kinetic study of molecular adsorption inside the porous film. As a continuous study, this work presents the broadening and the induced blue shift of the resonance band of the wavelength-interrogated PWMR sensor as well as its sensitivity to small molecule adsorption.

2 PREPARATION OF THE SENSOR

The gold-clad TiO_2 nanoporous waveguides were made in the same way as described in the previous work. Figure 1 shows the cross-sectional morphology of the waveguide chip observed by scanning electron microscopy (SEM). The TiO_2 film exhibits a random loose packing of TiO_2-nanoparticle aggregates (the particle diameter is ca. 6 nm), including the inter- and intra-aggregate pores. The cross section is rather coarse. The glass-substrate/gold-layer and gold-layer/TiO_2-film interfaces are clearly seen. The thicknesses of the gold layer and the nanoporous TiO_2 film were estimated as T_{Au} = 42.2 nm and T_{TiO2} = 310 nm.

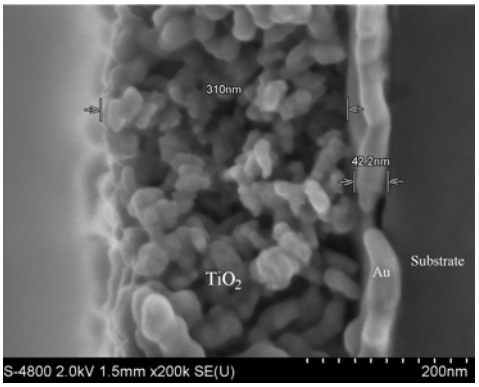

Figure 1: SEM image of the cross section of the waveguide

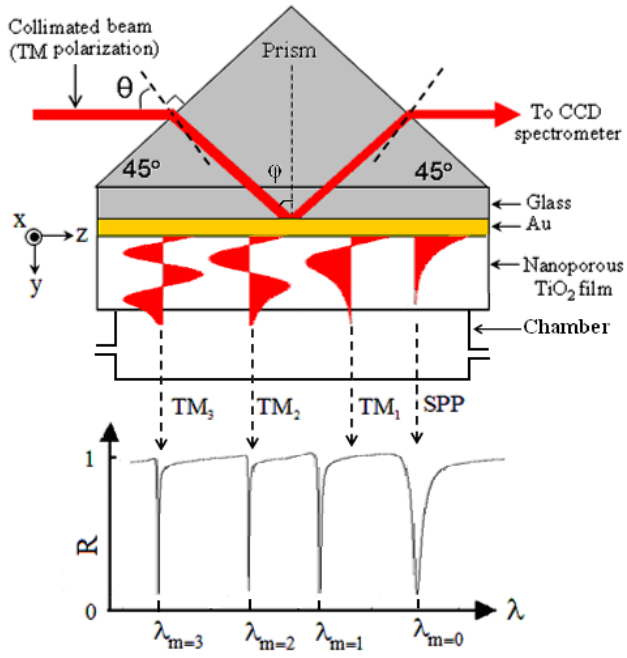

Figure 2: Schematic diagram of a wavelength-interrogated PWMR sensor (the TM mode profiles and the corresponding resonance bands were also illustrated).

Figure 2 displays the sensor configuration. It consists of a tungsten-halogen lamp, a CCD spectrum analyzer (Ocean Optics), a glass prism (45°/45°/90°, n_p = 1.799 at λ = 633 nm) and a slab waveguide chip that was tightly sandwiched between the prism and a fluidic chamber. Broadband light from the tungsten-halogen lamp passes through a quartz fiber, a linear polarizer and a lens, to produce a collimated beam with the *p*-polarization state. The beam is incident upon the prism at an angle θ (θ > 0 if the beam is between the glass substrate and the prism-surface normal, otherwise, θ < 0), undergoing attenuated total reflection (ATR) at the glass-substrate/gold-layer interface. ATR is accompanied by an evanescent field that penetrates through the gold layer to excite the guided modes in the TiO_2 film at specific wavelengths at which the phase-matching condition is satisfied. The energy transfer from the incoming light to the guided modes at the resonance wavelengths (λ_R) leads to ATR troughs in the reflected light intensity spectrum. Therefore, in principle λ_R and its shift induced by molecular adsorption can be determined by recording the reflected light intensity spectra with the CCD spectrometer

For understanding the PWMR sensor with wavelength interrogation, the profiles of transverse magnetic (TM) modes with different orders and the corresponding resonance bands in the reflectance spectrum were also illustrated in Figure 2. At a given incident angle, a higher-order mode has a smaller resonance wavelength. The TM_0 mode with the largest resonance wavelength corresponds to the surface plasmon polariton (SPP).

3 RESULTS AND DISCUSSIONS

Figure 3 displays a reflected light intensity spectrum detected at θ = 15° with the empty chamber. The spectrum was normalized to the peak intensity. It includes a single trough at λ_R=671 nm. The best fit to the measured spectrum was carried out using T_{Au} = 42.2 nm and T_{TiO2} = 310 nm based on the Fresnel equations. Prior to numerical calculations, the refractive-index (RI) dispersions of gold and TiO_2 were obtained and the average RI versus wavelength for nanoporous TiO_2 film was derived based on the Bruggeman approximation [7]. The best-fitting curve shown in Figure 3 leads to a pore-volume fraction of 0.474 for the prepared TiO_2 film. The further analyses based on waveguide theory indicate that the resonance band at λ_R=671 nm corresponds to the TM_1 mode. Compared with the best-fitting curve, the measured resonance band exhibits a considerable broadening that is mainly attributable to the

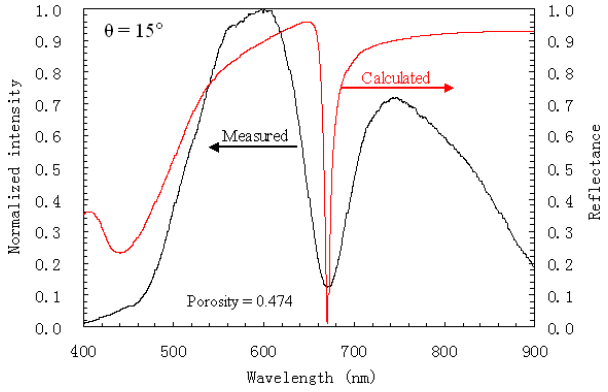

Figure 3: Reflected light intensity spectrum measured at θ = 15° with the air clad (the red curve is the best-fit result).

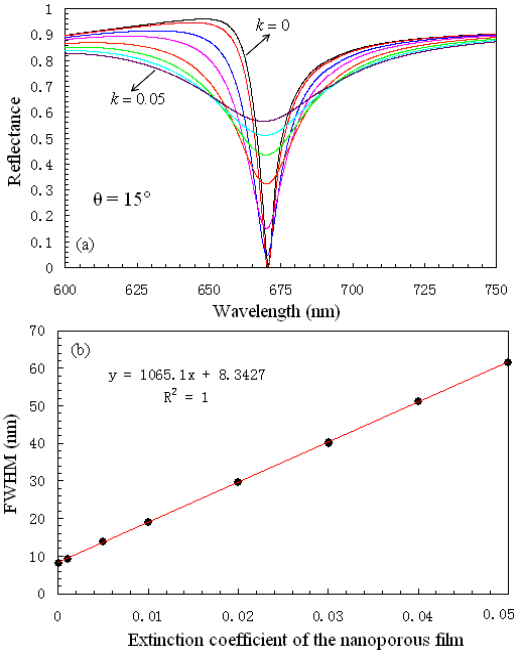

Figure 4: (a) Simulated reflectance spectra, (b) FWHM versus the extinction coefficient of the nanoporous layer

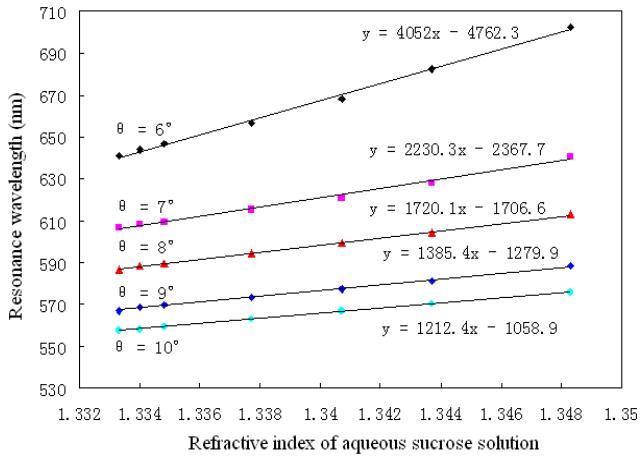

Figure 5: Resonance wavelengths versus refractive index of aqueous sucrose solution measured at different value of θ

the large scattering of the nanoporous TiO_2 film due to its coarse structure verified by SEM. The scattering induced broadening of the resonance band for the PWMR sensor was simulated by introduction of an extinction coefficient (k) to the nanoporous TiO_2 film. Figure 4(a) shows the reflectance spectra calculated with different values of k. The resonance band gradually widens with increasing k. Figure 4(b) shows that the full width at half maximum (FWHM) of the resonance band is linearly dependent on k. The resonance-band broadening weakens the spectral resolution, thus affecting the detection limit of the sensor.

The RI sensitivity of the PWMR sensor was examined using a series of aqueous sucrose solutions as the standard RI samples. Figure 5 shows the resonance wavelengths versus the solution RI measured at different incident angles. At a given θ λ_R linearly increases with increasing the solution RI from 1.333 to 1.348. The slope of the straight line, representing the RI sensitivity of the sensor, decreases with increasing the value of θ. Figure 5 also reveals that λ_R with water reduces with increasing θ. Therefore, it can be seen that the RI sensitivity of the sensor increases with increasing the initial resonance wavelength.

Response of the PWMR sensor to molecular adsorption was investigated at θ = 5° using the aqueous GSH solution samples. GSH is a small molecule composed of three amino acids with a molecular weight of 307.3 Da. Figure 6(a) shows the normalized intensity spectrum with water and that recorded at the equilibrium of GSH adsorption from the 0.1 mM solution. Adsorption of GSH molecules inside the nanoporous TiO_2 film leads to a redshift of $\Delta\lambda_R$ = 3 nm. According to dn/dc = 0.188ml/g [8], the RI difference between water and the 0.1 mM GSH solution is $\Delta n = 5.53 \times 10^{-6}$, it exceeds the detection limit of the sensor. Figure 6(b) displays the resonance-wavelength shifts versus the GSH concentrations measured at θ = 5°. As the concentration rises, $\Delta\lambda_R$ initially rises fast and then tends to be stable. Given RI =1.44 for GSH, the simulation results reveal that the volume fraction (Γ) for the GSH molecules adsorbed inside the nanoporous TiO_2 film is proportional to $\Delta\lambda_R$ with

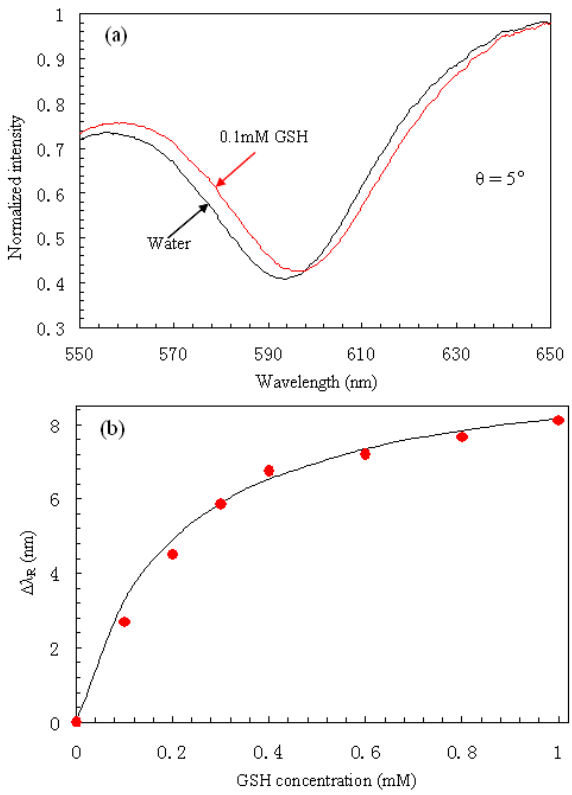

Figure 6: Reflected light intensity spectra corresponding to the water and aqueous GSH solution clads

$\Delta\Gamma/\Delta\lambda_R$ = 0.0173/nm. For the 1 mM GSH solution, $\Delta\lambda_R$ = 8.1 nm and Γ = 0.142. It suggests that even in the case of saturation adsorption the adsorbed GSH molecules only occupy 30% of the total pore volume.

As measured above, both changes in RI of the surrounding liquid and molecular adsorption usually lead to redshifts in the resonance band of the PWMR sensors. However, under proper conditions, the PWMR sensor can also produce blueshifts in the resonance band in response to adsorption of analyte molecules and changes in the liquid RI. Such a behavior of the PWMR sensor was theoretically demonstrated based on a nanoporous glass waveguide made of the same material as the prism used in this work. The theoretical calculations were carried out provided that the gold-clad layer is 30 nm, the nanoporous glass layer has a thickness of 2.6 μm and a pore-volume fraction of 0.4. Figure 7(a) shows the calculated reflectance spectra at the reflection angle of φ = 63.1°. As the liquid RI rises from n_c = 1.33 to 1.331, the resonance band gradually blueshifts from λ_R = 777.2 nm to 722.8 nm. Figure 7(b) shows a linear dependence of λ_R on n_c with the slope of $\Delta\lambda_R/\Delta n_c$ = –53482 nm/RIU. Namely, a 1nm blueshift of λ_R corresponds to $\Delta n_c = 1.87 \times 10^{-5}$.

To explain the resonance-band blueshift mechanism for the PWMR sensor based on the phase-matching condition, the effective RI dispersion of the guided mode in the porous glass waveguide was calculated using the above parameters. Figure 8 shows the calculated results. The two black curves

were obtained with n_c = 1.33 and 1.34. The red and blue curves were derived from the formula: $N = n_p \sin(\varphi)$, here φ = 63.1° and n_p is RI of the glass prism for the red curve and φ = 65.1° and n_p is RI of the Al_2O_3 crystal prism for the blue curve. There is a point of intersection between each black and each color curves, at which the phase matching appears between the in-coming light and the guided mode.

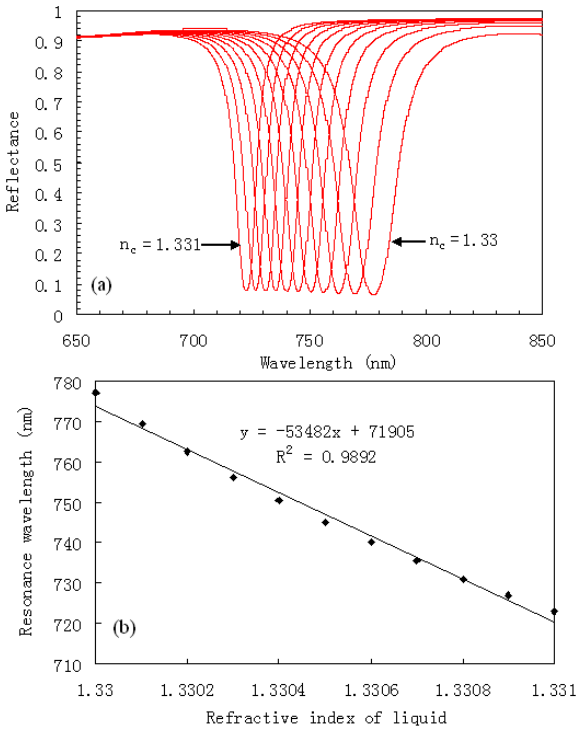

Figure 7: Reflected light intensity spectra corresponding to the water and aqueous GSH solution sample.

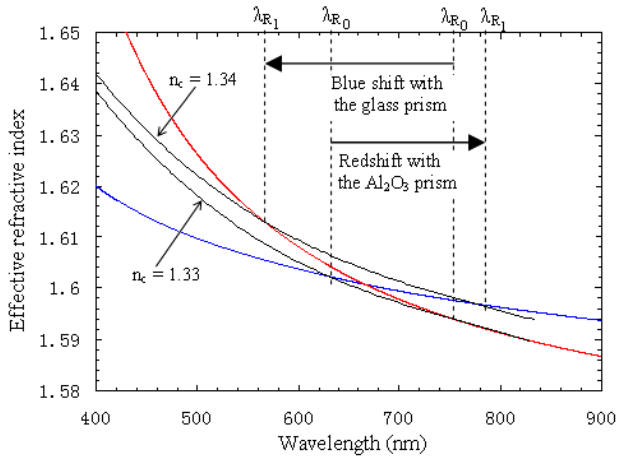

Figure 8: Wavelength dependence of the effective refractive index of the guided mode in the gold-clad nanoporous glass waveguide. The red and blue curves were described below.

The horizontal position of the intersection point is the resonance wavelength of the guided mode. Figure 8 clearly indicates that a change of n_c from 1.33 to 1.34 can lead to a blueshift in λ_R with the glass prism and a redshift with the Al_2O_3 crystal prism. The findings suggest that by use of a rutile prism to replace the glass prism, the nanoporous TiO_2 film based PWMR sensor could produce blue shifts in the resonance band in response to molecular adsorption and the liquid-RI changes.

4 CONCLUSIONS

The wavelength-interrogated PWMR sensors were prepared using the gold-clad nanoporous TiO_2 thin-film waveguides. The RI sensitivity of the sensor was examined to decrease from S = 4056 nm/RIU to 1212.4 nm/RIU with increasing the incident angles from θ = 6° to 10°. The resonance-band broadening of the sensor was observed and explained theoretically. The sensor was demonstrated to be responsive to small-molecule GSH adsorption. The pore-volume fraction of the TiO_2 film and that for the GSH molecules adsorbed inside the porous film were estimated by the best fitting to the experimental data. The theoretical analyses demonstrated that depending on the prism material used, a change in the liquid RI can cause not only a redshift but also a blueshift in the resonance band of the PWMR sensor. The PWMR sensor operating in the wavelength interrogation mode exhibits interesting behaviors and ultrahigh sensitivity to small-molecule targets.

ACKNOWLEDGEMENT

This work was supported by the National Natural Science Foundation of China (No. 60978042 and No. 61078039) and the National Basic Research Programme of China (No. 2009CB320300).

REFERENCES

[1] K. H. A. Lau, L. Tan, K. Tamada, M. S. Sander, W. Knoll, J. Chem. Phys. B, 108, 10812–10818, 2004.
[2] A. Yamaguchi, K. Hotta, N. Teramae, Anal. Chem., 81, 105-111, 2009.
[3] G. Rong, J. D. Ryckman, R. L. Mernaugh, S. M. Weiss, Appl. Phys. Lett., 93, 161109, 2008.
[4] Y. Jiao, S. M. Weiss, Biosens. Bioelectron., 25, 1535-1538, 2010
[5] Z. Qi, I. Honma, H. Zhou, Appl. Phys. Lett., 90, 011102, 2007.
[6] V. Hodnik, G. Anderluh, Sensors, 9, 1339-1354, 2009.
[7] A. Álvarez-Herrero, R. L. Heredero, E. Bernabeu, D. Levy, Appl. Opt. 40, 527-532, 2001.
[8] A. Brandenburg, R. Krauter, C. Künzel, M. Stefan, H. Schulte, Appl. Opt., 39, 6396-6405, 2000.